Intramolecular Borylation via Sequential B−Mes Bond Cleavage for the Divergent Synthesis of B,N,B-Doped Benzo[4]helicenes

Knöller, Julius A.; Meng, Guoyun; Wang, Xiang; Hall, David; Pershin, Anton; Beljonne, David; Olivier, Yoann; Laschat, Sabine; Zysman-Colman, Eli; Wang, Suning

Published in:
Angewandte Chemie. International edition

DOI:
10.1002/anie.201912340

Publication date:
2020

Document Version
Peer reviewed version

Intramolecular Borylation via Sequential B-Mes Bond Cleavage for the Divergent Synthesis of B,N,B-doped Benzo[4]helicenes

Julius A. Knöller[a,c], Guoyun Meng[b], Xiang Wang[a], David Hall[d,e], Anton Pershin[e], David Beljonne[e], Yoann Olivier[f], Sabine Laschat[c], Eli Zysman-Colman*[d], and Suning Wang*[a,b]

[a] J. A. Knöller, Dr. X. Wang, Prof. Dr. S. Wang, Department of Chemistry, Queen`s University, 90 Bader Lane, Kingston, Ontario, K7L 3N6, Canada, E-mail: sw17@queensu.ca
[b] G. Meng, Prof. Dr. S. Wang, School of Chemistry and Chemical Engineering, Beijing Institute of Technology, Beijing, China
[c] J. A. Knöller, Prof. Dr. S. Laschat, Institute for Organic Chemistry, Stuttgart University, Pfaffenwaldring 55, 70569 Stuttgart (Germany)
[d] D. Hall, Prof. Dr. E. Zysman-Colman, Organic Semiconductor Centre, EaStCHEM School of Chemistry, University of St Andrews, St Andrews, UK, KY16 9ST, E-mail: eli.zysman-colman@st-andrews.ac.uk
[e] A. Pershin, Prof. Dr. D. Beljonne, Laboratory for Chemistry of Novel Materials, University of Mons, 7000, Mons, Belgium.
[f] Dr. Y. Olivier, Unité de Chimie Physique Théorique et Structurale & Laboratoire de Physique du Solide, Namur Institute of Structured Matter, Université de Namur, Rue de Bruxelles, 61, 5000 Namur, Belgium.

Abstract: New symmetric and unsymmetric B,N,B-doped benzo[4]helicenes **3** - **6a/b** have been achieved in good yields, using a three-step process, starting from N(tolyl)3 in a highly divergent manner (7 examples). A borinic acid functionalized 1,4-B,N-anthracene **1** was found to display unprecedented reactivity, acting as a convenient and highly effective precursor for “one-pot” selective formation of various B,N,B-benzo[4]helicenes via intramolecular borylation and sequential B-Mes bond cleavage in presence of BBr3. Bromo substituted B,N,B-benzo[4]helicenes **2a**/**2b** were identified as the reactive intermediates, providing a highly effective toolbox for accessing symmetrically/unsymmetrically functionalized B,N,B-doped helicenes. Their high photoluminescence quantum yields along with the small ΔEST suggest the potential as thermally activated delayed fluorescence (TADF) emitters for organic light-emitting diodes (OLEDs).

Replacing carbon atoms in the framework of polyaromatic hydrocarbons with boron (B-PAHs) provides a viable strategy for the synthesis of numerous functional materials. Despite their great application potential e.g. in organic optoelectronics, chemical sensing and organocatalysis, systematic investigation of B-PAHs is hampered by complex synthetic methods, especially for implementation of multiple boron centers into one molecule.[1] Synthesis of B-PAHs typically relies on transmetallation[1c,2] and/or electrophilic aromatic substitution involving a strong electrophile (BCl3, BBr3), which is also referred to as Friedel Crafts borylation[1c,2b,4]. It has been shown that in Friedel Crafts borylations a bulky amine base NR3 binds the HX produced, and in combination with a Lewis acid e.g. AlCl3, activates the electrophile by forming borenium ions (R3N-B+X2).[3k] Most recently, triarylboranes BAr3 have been applied as H+ scavengers instead of NR3, improving the yield of the corresponding borylation reactions.[3d,3i] Other methods include Wacker type

cyclisations[4], hydroboration with NHC borenium ions[5] and construction of the targeted PAH framework around a pre-installed boron center via Yamamoto coupling[6a] or Scholl reactions[6b-c]. Pioneering work by Kawashima in the synthesis of 1,4-B,N-doped, linear acenes[2c-d,7a-b] for applications in OLEDs established the growing class of 1,4-azaborines[7]. Embedding 1,4-azaborine units into the scaffold of benzo[4]helicene (e.g. DABNA and *v*-DABNA in Scheme 1) by Hatakeyama et al. led to the discovery of multi-resonance TADF (MR-TADF) in 2016.[3h] In contrast to their charge transfer (CT) governed, donor-acceptor analogues[8], MR-TADF molecules exhibit a narrow □→□* emission band[3h], improving the color purity of the corresponding OLEDs significantly. Notably, only a few MR-TADF emitters are known so far and optimization of their photophysical properties relies on early stage introduction of donor units, which greatly hinders a systematic exploration of this new class of emitters.[3a,3d-e,3h] With the aim to achieve new B,N,B-doped helicenes such as **3** □ an inverted DABNA with respect to B and N positions (Scheme 1), we discovered a new and highly effective borylation method using 1,4-B,N-anthracene borinic acid **1** as the precursor, which enabled the synthesis of a series of symmetric and unsymmetric B,N,B-benzo[4]helicenes. The details are presented herein.

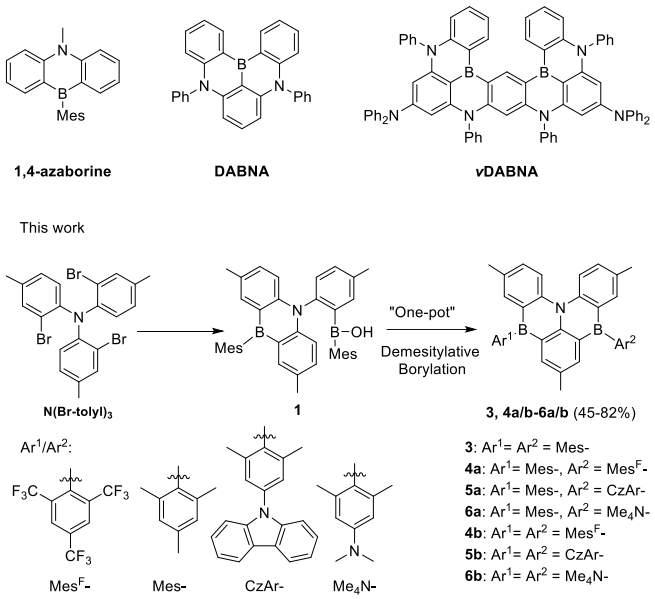

Scheme 1. Selected examples of 1,4-azaborine, B,N-benzo[4]helicene derivatives and the new borylation method for new B,N,B-benzo[4]helicenes.

The borinic acid **1** was prepared from readily available N(Br-tolyl)3 (Scheme 1) via transmetallation (*t*-BuLi and MesB(OMe)2 in THF, -78 °C) in 65% yield. The attempted conversion of **1** to **3** via an intramolecular Friedel Crafts borylation surprisingly led to the identification of the ring closed and demesitylated borinic acid **2a´** (Scheme 2) upon aqueous workup. To determine whether the B-Mes bond cleavage took place during the reaction or during the workup, the reaction of **1** with 1 equiv. BBr3 for 1 h (Scheme 2, Route A) was tracked via NMR, which in fact resulted in an unsymmetric, ring-closed B-Br compound **2a** and mesitylene[9a] as the main products (cf. supporting information, SI, section S3). Increasing the amount of BBr3 to 5 equiv. and the reaction time to 24 h (Scheme 2, Route B) led to the cleavage of the second B-Mes bond in **1** and the selective formation of the symmetric ring closed B-Br compound **2b**. NMR tracking at RT revealed a stepwise reaction where **2a** is formed first, supposedly via a demesitylative borylation and then converted to **2b** via B-Mes

bond cleavage and, surprisingly, a full conversion after 54 h (cf. SI, section S3). To rule out the acid dependency of the two B-Mes bond cleavages, the reaction in the presence of 2.5 equiv. DIPEA (di-*iso*propylethylamine) to scavenge any HBr formed was tracked by NMR (cf. SI, section S3). Astonishingly, the formation of **2a** still took place, albeit with Mes-BBr2[9b] as the by-product instead of mesitylene, indicating a complicated reaction mechanism. The conversion of **2a** to **2b** however was inhibited by DIPEA, supporting that the second Mes group likely acts as an intramolecular H+ scavenger, in a manner similar to the previously reported reactivity of BAr3 as an additive in Friedel Crafts Borylations.[3d,3i]

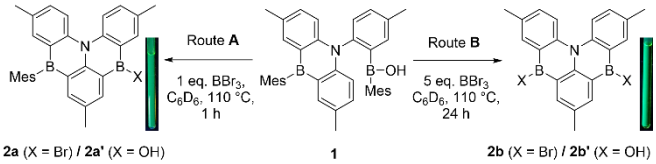

Scheme 2. Route **A**: formation of the unsymmetric ring-closed B-Br **2a** and the borinic acid **2a′**, Route **B**: formation of the symmetric ring-closed B-Br **2b** and the borinic acid **2b′**. The B-Br intermediates **2a** and **2b** were identified via NMR, and further verified by identification of the ring-closed borinic acids **2a′** and **2b′** via HRMS upon aqueous workup. Insets: photographs showing the characteristic fluorescence colour of **2a** and **2b** (λ_{exc} = 366 nm).

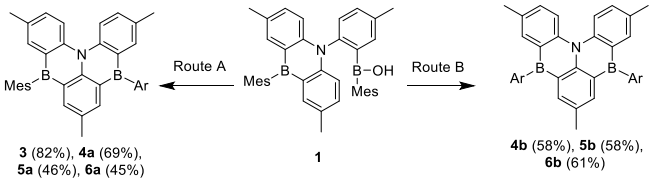

Scheme 3. Route A: Synthesis of **3** and the unsymmetric B,N,B helicenes **4a** - **6a**: 1) BBr_3 (1 equiv.), toluene, 110 °C, 1 h, 2) Ar-Li (1.2 equiv.), THF or Et_2O, -78 °C to r.t., 12 h. Route B: Synthesis of the symmetric derivatives **4b** - **6b**: 1) BBr_3 (5 equiv.), toluene, 110 °C, 24 h, 2) Ar-Li (2.4 equiv.), THF or Et_2O, -78°C to r.t., 12 h. Reactions were performed in sealed tubes and volatiles were removed between steps 1) and 2).

After establishing the reaction conditions for selective formation of symmetric and unsymmetric B,N,B-intermediates **2a**/**b**, compounds **3**, and **4a**/**b** to **6a**/**b** were prepared from **1** using Route A and B, respectively (Scheme 3), in a “one pot” manner. For example, after the formation of **2a**, the addition of Mes-Li (Route A) resulted in the isolation of the B,N,B-doped helicene **3** as a yellow solid in an excellent yield of 82%. Replacing Mes-Li with the desired Ar-Li via Route A or B, 3 pairs of B,N,B-helicenes **4a/b** - **6a/b** were isolated in 45% to 69% yields. The Ar-Li compounds were readily accessible via lithium-halide exchange protocols[2a,2c,10], or in the case of fluoromesityl (MesF), via deprotonation of a C-H bond[13a]. Notably, during our investigation, the synthesis of **3** was published in a patent by Hatakeyama et al.[11], which relies on a one-pot transmetallation/ Friedel Crafts borylation yielding **3** in 22% yield. Our methodology allows not only the preparation of **3** in a much higher overall yield (22% vs. 53%, starting from N(Br-tolyl)3), but also the symmetric and unsymmetric decoration of the B,N,B-doped backbone in a highly divergent manner.

All B,N,B-benzo[4]helicenes and the precursor **1** are air stable and fully characterized by NMR, HRMS, and except for **5b** and **6a**, by single-crystal X-Ray diffraction analyses (cf. SI, section S9). Compound **3** exhibits helical chirality in the solid state (Figure 1a) with both enantiomers present in the unit cell. The dihedral angle between the peripheral tolyl rings (49.4 °) in **3** is much larger than that of [4]helicene (24.9 °)[12a-b] and between those of [5]helicene (46.0 °)[12c] and [6]helicene (58 °)[12a-b]. Longer B-C bonds (1.523(2) Å - 1.572(1) Å) in **3** compared to the C-C bonds (1.33 Å - 1.44 Å)[12d] in [4]helicene push the tolyl rings closer, giving rise to the increased distortion. The B-C bonds as well as the N-C bonds are typical single bonds[3d], rendering the central BNC4 units non-aromatic, in accordance with slightly positive NICS(0) values of 1.3 and 1.5 (cf. SI, Figure S82). Unsymmetric and symmetric functionalization resulted in similar structural features with dihedral angles of the tolyl rings between 50.2° (**4a**) and 53.3° (**5a**). Notably, as shown by the structure of **4a** (Figure 1b), the MesF derivatives **4a/b** exhibit short B-F contacts, similar to those reported by Jäkle and Marder et al.[13]

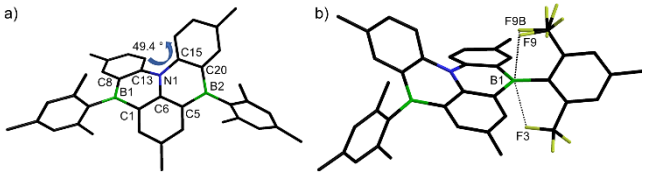

Figure 1. a) Crystal structure of **3** with selected bond lengths [Å]: B1-C1 1.532(2), B1-C8 1.572(1), B1-C22 1.534(1), B2-C5 1.562(1), B2-C15 1.539(2), B2-C31 1.566(1), N1-C6 1.414(1), N1-C13 1.422(1), N1-C20 1.417(1), C1-C6 1.396(1), C5-C6 1.423(1), C8-C13 1.461(1), C15-C20 1.411(1); b) Crystal structure of **4a** showing the rotational disorder of the CF_3 group and the short B-F contacts [Å]: B1-F3 2.655(2), B2-F9 2.551(7), B2-F9B 2.539(5). Hydrogen atoms are omitted for clarity.

Investigation of the photophysical properties of **3** - **6a/b** (Table 1, cf. SI, section S6) revealed only minor influence of the B functionalization on the absorption spectra (λabs = 458 nm - 461 nm) as shown by **3** and **6b** in Figure 2a. Computational studies via TD-DFT and, for the symmetric derivatives **3**, **4a**, **5b** and **6b** additionally by the more accurate SCS-CC2 method[14] (Figure 2; cf. SI, section S7 – S8,) suggest that the narrow absorption bands are 𝜋→𝜋* transitions in the B,N,B-doped backbone and are comprised of the HOMO to LUMO transition for **3** and HOMO-2 to LUMO transition for **6b** with high oscillator strengths. DFT calculations suggest HOMO/ HOMO-1 of **6b** being localized on the amino donor, resulting in small oscillator strengths (f = 0.003 and 0.000) for the corresponding CT transitions, consistent with their absence in the absorption spectrum.

Table 1. Selected photophysical and electrochemical properties of the B,N,B-doped helicenes **3**, **4a/b** - **6a/b**

	Photophysical				Electrochemical	
Cmpd.	λ_{abs} [nm][a]	λ_{em} [nm][a]	Φ [%][b]	ΔE_{ST} [eV][c]	E_{HOMO} [eV][d]	E_{LUMO} [eV][d]

	(ε [M^{-1} cm^{-1}])					
3	458 (26000)	482	71	0.18	−5.62	−2.55
4a	458 (25000)	485	88	0.19	−5.69	−2.69
4b	459 (23000)	487	85	0.19	−5.79	−2.76
5a	460 (29000)	483	82	0.18	−5.61	−2.64
5b	461 (31000)	486	81	0.17	−5.61	−2.71
6a	460 (23000)	477, 609	19	0.17	−5.05	−2.54
6b	461 (26000)	481, 601	18	0.13	−5.06	−2.53

[a] in CH_2Cl_2 ($c = 2 \times 10^{-5}$ mol L^{-1}, λ_{exc} = 435 nm), [b] in N_2-saturated CH_2Cl_2 ($c = 2 \times 10^{-5}$ mol L^{-1}) using an integration sphere, [c] determined from the fluorescence maxima λ_F at 298 K and the phosphorescence maxima λ_P at 77 K measured in a 1 wt% PMMA film: $\Delta E_{ST} = 1240/\lambda_F - 1240/\lambda_P$, [d] $E_{HOMO/LUMO}$ calculated from $E_{ox/red}$ ($E_{HOMO/LUMO} = -(4.8\ eV + E_{ox/red})$, E_{ox} and E_{red} were determined from the first oxidation/ reduction peak in DPV diagrams recorded in 2 mM solutions of the analyte in dry and N_2 saturated CH_2Cl_2/ THF (**6a/b** in THF only), with $^nBu_4PF_6$ (0.1 mM) as the electrolyte, scan rate 100 mV s^{-1}, potential referenced vs. Fc/ Fc^+.

The narrow emission band of **3** (λem = 482 nm, λ = 71%) with a small Stokes shift of 1087 cm-1 corresponds to a small geometrical reorganization similar to that predicted for DABNA-1.[14] Functionalization with electron-withdrawing MesF (**4a/b**) results in similar emission properties in accordance to computational results, and higher luminescence quantum yields of 88%/ 85% for **4a**/**b**. The increase of Φ can be rationalized by suppressed vibrational modes of the C-F bonds and rigidification through previously mentioned, weak B-F interactions. The carbazolyl derivatives **5a/b** exhibit similar emission features to **3**, e.g. small stokes shifts of 1035 cm-1/1116 cm-1, and high Φ of 82% / 81%, respectively, in agreement with the SCS-CC2 calculations.[14] In contrast, the amino functionalized compounds **6a**/**b**

show an interesting dual emission as shown by **6b** in Figure 2a. The dominating, broad emission (λem = 601 nm) typical for the geometrical reorganization of CT molecules[8,14] suggests a transition from the amino centered HOMO to the B,N,B-backbone centered LUMO (Figure 2b) in accordance to the TD-DFT results for **6b**. The minor emission (λem = 481 nm) likely originates from the $\pi \rightarrow \pi^*$ transition in the B,N,B-backbone. A similar behavior of **6a** (λem = 609 nm, 477 nm) further supports the transformation of **6a**/**b** to CT-dominated molecules upon introduction of the amino group, which is contrary to the SCS-CC2 calculated data (Figure 2c). Investigation of the solvatochromism supports our assignment of electronic transitions in **3** - **6a/b** (cf. SI, section S6). Significantly, the donor functionalized molecules **5a/b** and **6a/b** display a sharp increase of emission intensity with increasing temperature (T), in stark contrast to **3** that decreases in emission intensity with increasing T. Determination of the singlet-triplet energy gap Δ*E*ST (Table 1) in 1 wt% PMMA film
revealed small Δ*E*ST values ranging between 0.13 eV for **6b** and 0.19 eV for **4a/b** (Table 1) in agreement to the MR structure of **3** - **5a**/**b** as visualized by the computed difference density in the excited states[14] (Figure 2c) and the CT structure[8] of **6a**/**b**.

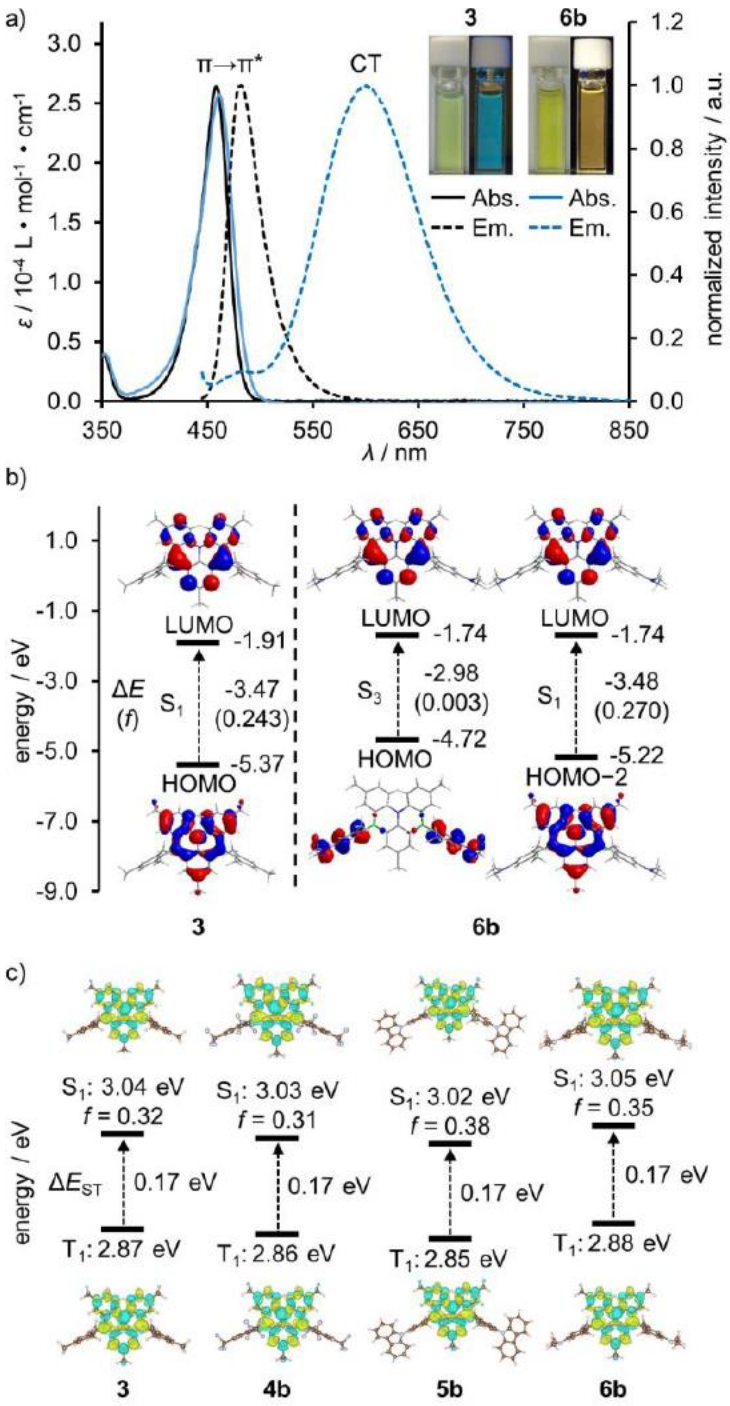

Figure 2. a) UV/Vis absorption and emission spectra of **3** and **6b** in CH2Cl2 (c = 2 × 10-5 mol L-1, λex = 435 nm), insets: photographs showing the corresponding (fluorescence) colour (λex = 366 nm); b) S1 and S1/S3 vertical excitations for **3** and **6b** with excitation energies, oscillator strengths and contributing orbitals (B3LYP/ 6-31G(d), a = 0.03); c) S1/ T1 vertical excitation energies, oscillator strengths and difference density maps for **3**, **4b** - **6b** (SCS-CC2, cc-pVDZ). Blue/ green indicates decrease/ increase of e- density.

Electrochemical analysis of the B,N,B-heterocycles (Table 1, cf. SI, Figure S81) showed reversible oxidation/ reduction with only the oxidation of **5a**/**b** being irreversible, presumably caused by electro-oligomerization[15] of the carbazolyl side groups. The trend of the extracted HOMO/ LUMO energies (*E*HOMO/ *E*LUMO) is in good agreement with the DFT

results (cf. SI, Table S4). For example, introduction of MesF groups in **4a**/**b** subsequently lowers *E*LUMO to -2.69 eV / -2.76 eV, compared to **3** (*E*LUMO = -2.55 eV), rendering **4a**/**b** as potential electron acceptors in optoelectronics. The significant difference in *E*HOMO for **6a**/**b** (-5.05 eV/ -5.06 eV) compared to that of **3** arises from the localization of the HOMOs on the amino groups, in agreement with the computational and experimental data.

In summary, 1,4-B,N-anthracene borinic acid **1** has been found to display a previously unknown reactivity, undergoing an intramolecular borylation and sequential B-Mes bond cleavage to form **2a**/**b**. This reaction proceeds slowly at RT and accelerates at high T, which could pave the way for new, milder procedures in the preparation of B-doped PAHs with high yields and functional group tolerance. Furthermore, the potential of this B-PAH synthesis has been demonstrated by the successful and highly divergent synthesis of a series of B,N,B-doped benzo[4]helicenes. These new highly fluorescent compounds are promising candidates as TADF emitters for OLEDs. Further investigation of the reaction mechanism and the substrate scope are currently undertaken in our laboratory.

Acknowledgements

We thank the Natural Sciences and Engineering Research Council of Canada and the Leverhulme Trust (RPG-2016-47) for financial support. J. A. Knöller thanks the Baden Württemberg Stiftung for a scholarship as well as Queen`s and Stuttgart University for enabling this research through the Dual Degree Masters program.

Keywords: synthetic methods • boron • luminescence • heterocycles • divergent synthesis

[1] a) M. Hirai, N. Tanaka, M. Sakai, S. Yamaguchi, *Chem. Rev.* **2019**, *119*, 8291–8331; b) S. K. Mellerup, S. Wang, *Trends Chem.* **2019**, *1*, 77–89; c) E. von Grotthuss, A. John, T. Kaese, M. Wagner, *Asian J. Org. Chem.* **2018**, *7*, 37–53; d) L. Ji, S. Griesbeck, T. B. Marder, *Chem. Sci.* **2017**, *8*, 846–863; e) A. Escande, M. J. Ingleson, *Chem. Commun.* **2015**, *51*, 6257–6274; f) F. Jäkle, *Chem. Rev.* **2010**, *110*, 3985–4022.

[2] a) T. L. Wu, M. J. Huang, C. C. Lin, P. Y. Huang, T. Y. Chou, R. W. Chen-Cheng, H. W. Lin, R. S. Liu, C. H. Cheng, *Nat. Photonics* **2018**, *12*, 235–240; b) A. John, M. Bolte, H. Lerner, M. Wagner, *Angew. Chem. Int. Ed.* **2017**, *56*, 5588–5592; *Angew. Chem.* **2017**, *129*, 5680– 5684; c) L. G. Mercier, W. E. Piers, M. Parvez, *Angew. Chem. Int. Ed.* **2009**, *48*, 6108–6111; *Angew. Chem.* **2009**, *121*, 6224–6227; d) T. Agou, J. Kobayashi, T. Kawashima, *Chem. Commun.* **2007**, 3204– 3206; e) T. Agou, J. Kobayashi, T. Kawashima, *Org. Lett.* **2006**, *8*, 2004–2007.

[3] a) Y. Kondo, K. Yoshiura, S. Kitera, H. Nishi, S. Oda, H. Gotoh, Y. Sasada, M. Yanai, T. Hatakeyama, *Nat. Photonics* **2019**, DOI 10.1038/s41566-019-0476-5; b) G. Meng, X. Chen, X. Wang, N. Wang, T. Peng, S. Wang, *Adv. Opt. Mater.* **2019**, *7*, 1–14; c) S. Nakatsuka, N. Yasuda, T. Hatakeyama, *J. Am. Chem. Soc.* **2018**, *140*, 13562–13565; d) K. Matsui, S. Oda, K. Yoshiura, K. Nakajima, N. Yasuda, T. Hatakeyama, *J. Am. Chem. Soc.* **2018**, *140*, 1195–1198; e) X. Liang, Z. P. Yan, H. B. Han, Z. G. Wu, Y. X. Zheng, H. Meng, J. L. Zuo, W. Huang, *Angew. Chem. Int. Ed.* **2018**, 11486–11490; *Angew. Chem.* **2018**, *130*, 11486–11490; f) D. T. Yang, T. Nakamura, Z. He, X. Wang, A. Wakamiya, T. Peng, S. Wang, *Org. Lett.* **2018**, *20*, 6741–6745; g) S. Nakatsuka, H. Gotoh, K. Kinoshita, N. Yasuda, T. Hatakeyama, *Angew. Chem. Int. Ed.* **2017**, *56*, 5087–5090; *Angew. Chem.* **2017**, *129*, 5169– 5172; h) T. Hatakeyama, K. Shiren, K. Nakajima, S. Nomura, S. Nakatsuka, K. Kinoshita, J. Ni, Y. Ono, T. Ikuta, *Adv. Mater.* **2016**, *28*, 2777–2781; i) M. Numano, N. Nagami, S. Nakatsuka, T. Katayama, K. Nakajima, S. Tatsumi, N. Yasuda, T. Hatakeyama, *Chem. - A Eur. J.* **2016**, *22*, 11574–11577; j) H. Hirai, K. Nakajima, S. Nakatsuka,

K. Shiren, J. Ni, S. Nomura, T. Ikuta, T. Hatakeyama, *Angew. Chem. Int. Ed.* **2015**, *54*, 13581–13585; *Angew. Chem.* **2015**, *127*, 13785–13789; k) M. J. Ingleson, *Synlett* **2012**, *23*, 1411–1415; l) T. Hatakeyama, S. Hashimoto, S. Seki, M. Nakamura, *J. Am. Chem. Soc.* **2011**, *133*, 18614–18617..
[4] T. Kaehler, M. Bolte, H.-W. Lerner, M. Wagner, *Angew. Chemie Int. Ed.* **2019**, *58*, 11379–11384.
[5] a) M. Farrell, C. Mu, D. Bialas, M. Rudolf, K. Menekse, A. Krause, M. Stolte, F. Würthner, *J. Am. Chem. Soc.* **2019**, *141*, 9096–9104: b) J. M. Farrell, D. Schmidt, V. Grande, F. Würthner, *Angew. Chem. Int. Ed.* **2017**, *56*, 11846–11850; *Angew. Chem.* **2017**, *129*, 12008–12012.
[6] For Yamamoto coupling refer to: a) K. Schickedanz, T. Trageser, M. Bolte, H. Lerner, M. Wagner, *Chem. Commun.* **2015**, *51*, 15808–15810; for Scholl reactions refer to: b) C. Dou, S. Saito, K. Matsuo, I. Hisaki, S. Yamaguchi, *Angew. Chem. Int. Ed.* **2012**, *51*, 12206–12210; *Angew. Chem.* **2012**, *124*, 12372–12376; c) S. Saito, K. Matsuo, S. Yamaguchi, *J. Am. Chem. Soc.* **2012**, *134*, 9130–9133.
[7] a) T. Agou, M. Sekine, J. Kobayashi, T. Kawashima, *J. Organomet. Chem.* **2009**, *694*, 3833–3836; b) T. Agou, M. Sekine, J. Kobayashi, T. Kawashima, *Chem. Commun.* **2009**, 1894–1896; c) M. Ando, M. Sakai, N. Ando, M. Hirai, S. Yamaguchi, *Org. Biomol. Chem.* **2019**, *17*, 5500–5504; d) Z. X. Giustra, S. Y. Liu, *J. Am. Chem. Soc.* **2018**, *140*, 1184– 1194; e) G. Bélanger-Chabot, H. Braunschweig, D. K. Roy, *Eur. J. Inorg. Chem.* **2017**, *2017*, 4353–4368; f) J. Y. Wang, J. Pei, *Chinese Chem. Lett.* **2016**, *27*, 1139–1146.
[8] a) H. Uoyama, K. Goushi, K. Shizu, H. Nomura, C. Adachi, *Nature* **2012**, *492*, 234–238; b) T. T. Bui, F. Goubard, M. Ibrahim-Ouali, D. Gigmes, F. Dumur, *Beilstein J. Org. Chem.* **2018**, *14*, 282–308; c) Y. Liu, C. Li, Z. Ren, S. Yan, M. R. Bryce, *Nat. Rev. Mater.* **2018**, *3*, 18020; d) M. Y. Wong, E. Zysman-Colman, *Adv. Mater.* **2017**, *29*, 160544.
[9] For chemical shifts of Mes-H refer to SI of: a) A. W. Wong, K. L. Miller, P. L. Diaconescu, *Dalt. Trans.* **2010**, *39*, 6726–6731; For chemical shifts of Mes-BBr2 refer to: b) A. Sundararaman, F. Jäkle, *J. Organomet. Chem.* **2003**, *681*, 134–142.
[10] a) S. Wiedbrauk, B. Maerz, E. Samoylova, A. Reiner, F. Trommer, P. Mayer, W. Zinth, H. Dube, *J. Am. Chem. Soc.* **2016**, *138*, 12219–12227.
[11] T. Hatakeyama, K. Matsui, Y. Watanabe, D. Baba, Y. Sasada, M. Yanai, T. Ikuta, *International Patent No. WO2018047639*, **2018**.
[12] a) Y. Shen, C. F. Chen, *Chem. Rev.* **2012**, *112*, 1463–1535; b) R. H. Martin, *Angew. Chemie Int. Ed.* **1974**, *13*, 649–660; c) V. Berezhnaia, M. Roy, N. Vanthuyne, M. Villa, J. V. Naubron, J. Rodriguez, Y. Coquerel, M. Gingras, *J. Am. Chem. Soc.* **2017**, *139*, 18508–18511; d) F. L. Hirshfeld, S. Sandler, G. M. J. Schmidt, *J. Chem. Soc.* **1963**, 2108–2125.
[13] a) X. Yin, J. Chen, R. A. Lalancette, T. B. Marder, F. Jäkle, *Angew. Chem. Int. Ed.* **2014**, *53*, 9761–9765; *Angew. Chem.* **2014**, *126*, 9919– 9923; b) Z. Zhang, R. M. Edkins, M. Haehnel, M. Wehner, M. Meier, J. Brand, H. Braunschweig, T. B. Marder, *Chem. Sci.* **2015**, *6*, 5922–5927.
[14] A. Pershin, D. Hall, V. Lemaur, J. C. Sancho-Garcia, L. Muccioli, E. Zysman-Colman, D. Beljonne, Y. Olivier, *Nat. Commun.* **2019**, *10*, 1–5.
[15] R. Stahl, C. Lambert, C. Kaiser, R. Wortmann, *Chem. Eur. J.* **2006**, *12*, 2358–2370.